

**Biosynthesis and characterization of silver nanoparticles produced by plant extracts and its antimicrobial activity**

**Abstract**

*Solanum tubersum* is the fourth most imperative plant in Egypt that is affected by numerous, fungi, viral and bacterial diseases. Bacterial and fungal isolates were collected and main pathogens were existing; Brown rot disease (*Ralstonia solaniserum*), soft root disease (*Pectobacterium carotovora*) and dry rot disease (*Fusarium oxisporum*). The green extracts of silver nanoparticles were prepared by means of aqueous extracts of three wild plants, *Physalis peruviana* (leaves, red and green fruits) (N1, N2 and N3), *Solanum nigrum* (fruit) (N4) and *Moringa oliefera* (leaves) (N5). The characterization of the biosynthesis of silver nanoparticles was achieved via SEM, TEM, FT-IR and X-RD, and the resulting nanoparticles were spherical, smooth and appeared to differ in size from 12 to 33 nm. The activity of the nanoparticle formulations was tested against the two bacterial isolates using agar diffusion method and one fungus using mycelial growth method. For the five formulations, N5 formulation exerted significantly potent antibacterial activity against *R. solanacearum*. Nevertheless, N1 formulation was the highest active one against *P. carotovra*. In addition, the antifungal activity indicated that N1 had the highest effect ( $EC_{50} = 687.03$  mg/L) followed by N3 ( $EC_{50} = 981.61$  mg/L) against *F. oxysporium*. Nanoparticles synthesized by wild plants could be used as safe alternatives to harmful microbicides.

**Keywords:** Biosynthesis, Silver nanoparticles, *Physalis peruviana*, *Solanum nigrum*, *Moringa oliefera*, Plant extract, Antifungal, Antibacterial, SEM, TEM, FT-IR, XRD.

**1. Introduction**

*Solanum tubersum* (family Solanaceae) is a worldwide-cultivated tuber-bearing plant, which is the fourth main food crop in the world after rice (*Oryza sativa*), maize (*Zea mays*) and wheat (*Triticum aestivum*), in terms of both area cultivated and total production (Douches et al., 1996). Potato does not require special growth conditions; it has been for a long time a major field crop in temperate regions, and increasingly in warmer regions (Haverkort, 1990). It is currently the second most important vegetable crop after tomatoes in Egypt, and Egypt is one of Africa's largest potato producers and exporters. Potato is susceptible to a number of diseases, including late blight caused by *Phytophthora infestans*, several viruses and bacterial wilt caused by *Ralstonia solanacearum*. Bacteria and Fungi are played a major role in the yield losses,

36 especially *Erwinia* the causal agent of soft rot in potato (**Rashid et al. 2012**) and *Alternaria spp*  
37 the causal agent of early blight of potato (**Belosokhov et al., 2017**). *Ralstonia solanacearum*, the  
38 causative agent of bacterial wilt in potatoes, is soilborne and can persist in soil for a long time in  
39 infected host plant debris or by colonizing potato volunteer plants, alternative hosts or even non-  
40 host plants (**Aliye et al., 2008**). To infect a plant successfully, the pathogen first has to be able to  
41 penetrate and colonize host tissues and overcome active plant defense responses to induce the set  
42 of events finally that leads to disease symptoms. Additionally, *Pectobacterium carotovra* is a  
43 gram-negative phytopathogenic bacterium, which attack several of plants such as carrots,  
44 potatoes, cucumber, onions and tomatoes. It caused black leg (soft rot) to these plants during  
45 cultivation, transportation and storage (**Leite et al., 2014**). *Pectobacterium* caused destruction of  
46 the cell wall of the plants then cause death of the plants. Fusarium wilt diseases are responsible  
47 for important yield losses on numerous crops. *Fusarium oxysporum* causes dry rot, stem-end rot  
48 and wilt of potatoes (*Solanum tuberosum L.*). Fusarium dry rot is mainly a post-harvest disease  
49 and can become a major problem when infected potatoes are stored. Chemical control of potato  
50 brown rot with currently available crop protectants is not effective (**Lopez and Biosca, 2004**).  
51 Development of more effective chemical control methods is not encouraged due to the general  
52 awareness about negative impacts of synthetic crop protectants on human health and the  
53 environment; this has led to the phasing out of an increasing number of crop protectants.  
54 Therefore, there is a clear need to develop alternative practical, safe and effective management  
55 strategies that can shorten the time that host plants can be grown. Plant extracts of many  
56 higher plants have been reported to exhibit antibacterial and antifungal properties under  
57 laboratory trails (**Okigbo and Ogbonnaya, 2006; Shariff et al., 2006**). Plant metabolites and  
58 plant-based pesticides appear to be one of the better alternatives as they are known to have  
59 minimal environmental impact and danger to consumers in contrast to the synthetic pesticides  
60 (**Varma and Dubey, 1999**). Nanotechnology has been used on widespread in plant pathogens  
61 and the application of nanoparticles become important in the management of plant diseases  
62 (**Sastry et al., 2010**). Biosynthesized of silver nanoparticles using plant extracts are an important  
63 contrast chemical and biosynthetic using platinum, silver and gold in the synthesized of  
64 nanoparticles (**Patil and Hooli, 2013**). Therefore, the present study aims to synthesize silver  
65 nanoparticles by a green biological route, using an extract derived from *Physalis peruviana*  
66 (leaves, red and green fruits), *Solanum nigrum* (fruit) and *Moringa oliefera* (leaves).  
67 Characterization of the synthesized nanoparticles performed using scanning electron microscope  
68 (SEM), transmission electron microscope (TEM), X-ray diffraction (XRD) and Fourier transform  
69 infrared spectroscopy (FT-IR) analysis. Besides, their antimicrobial activity against  
70 representatives of plant pathogenic bacteria (*Pectobacterium carotovra* and *Ralstonia*  
71 *solaniserum*) and fungus (*Fusarium oxysporium*) was investigated.

72

73

74

## 75 2. Materials and methods

### 76 2.1. Cultures and growth conditions

77 The potato plants were grown at two localities in Abo-Homous and Borg-Elarb, El-Behera  
78 and Alexandria Governorates, respectively, Egypt during the growing season 2016. The two  
79 bacteria were isolated from infected potato tubers and purified on Luria Bertani medium (LB)  
80 (Maniatis et al. 1982), and incubated for 24 hours at 30°C. In addition, the fungi was grown on  
81 Potato dextrose agar (PDA) and Kelman's TZC media (Kelman, 1954), then incubated at 28°C  
82 for 7 days. The microbes (bacteria and fungi) were identified using different methods including  
83 microscopically extension and molecular identification.

### 84 2.2. Pathogenicity test

85 According to (Zhang et al., 2014) with some modification, healthy potato tubers selected  
86 and washed carefully in water. Then tubers dipped in ethanol 70% for 5 min and washed in  
87 distilled water. Sterilized tuber was inoculated by syringe in plates containing a piece of sterile  
88 cotton saturated with water. The suspension concentration of bacteria and fungi were  $10^8$  and  $10^6$   
89 CFU/mL, respectively. Control tubers were inoculated by distilled water and incubated at the  
90 same conditions.

### 91 2.3. Preparation of the plant extracts

92 Three medicinal plants, *P. peruviana* (leaves, red and green fruits), *S. nigrum* (fruit) and  
93 *M. oliefera* (leaves) were selected from Abo-Homous and Borg-Elarb, El-Behera and Alexandria  
94 Governorates, respectively, Egypt. Fresh and healthy leaves and fruits were collected locally and  
95 rinsed thoroughly first with tap water followed by distilled water to remove all the dust and  
96 unwanted visible particles, cut into small pieces and dried at room temperature. About 10 g of  
97 these finely incised leaves of each plant type were weighed separately, 100 mL distilled water  
98 was added and boiled for about 20 min. The extracts were then filtered thrice to get clear  
99 solutions, which were then, refrigerated (4°C) for further experiments (Banerjee et al., 2014).

### 100 2.4. Green synthesis of silver nanoparticles formulations

101 Plant extract was added to aqueous solution (10 mM) of silver nitrate ( $\text{AgNO}_3$ ) in dark flask  
102 with shaking at 250 rpm and the changes in the color was observed. The reduction of Ag solution  
103 was subjected to UV- Visible spectrophotometer at 540 nm (Beckman, model Du 540), and the  
104 reaction stopped when the value of optical density was decreased. The solution was centrifuged  
105 at 12000 rpm for 30 min, the supernatant was discard and the pellet washed 3 times by sterile  
106 water. The pellet was dried at 50°C and then dissolved in sterile water (Banerjee et al., 2014).

### 107 2.5. Characterization of silver nanoparticles formulations

### 108 **2.5.1. Scanning electron microscopy (SEM)**

109 Scanning electron microscopy (SEM) is a method for high-resolution imaging of surfaces.  
110 SEM analysis was done by using a JEOL JSM-5410 (Japan) electron microscope with a W-  
111 source and operating at 80 kV. Sample was prepared on a glass slide (1 × 1 cm) after washing it  
112 with ethanol. A tiny drop of nanoparticles was spreaded evenly over glass slide and allowed to  
113 air dry. In order to make it conductive, gold coating with Jeol Quick Auto Coater was performed  
114 (JFC-1500). The NPs were then subjected to SEM analysis under ambient conditions.

### 115 **2.5.2. Transmission electron microscopy (TEM)**

116 Morphology of the nanoparticles usually determined by transmission electron microscopy  
117 (TEM). A combination of bright-field imaging at increasing magnification and of diffraction  
118 modes use to reveal the form and size of the nanoparticles. To perform the TEM observations,  
119 the nanoparticles formulation dilute with water (1/100). A drop of the diluted nanoparticles  
120 directly deposited on the film grid and observed after dry.

### 121 **2.5.3. Fourier transform infrared spectroscopy (FT-IR)**

122 FTIR spectra of nanoparticles were taken with potassium bromide pellets on a Thermo  
123 Nicolet AVATAR 300 FTIR spectrometer in the range 400-4000  $\text{Cm}^{-1}$ .

### 124 **2.5.4. X-ray diffraction analysis (XRD)**

125 X-ray powder diffraction patterns of nanoparticles were obtained by a D/max-rA  
126 diffractometer. The X-ray source was CuK radiation (40 kV, 80 mA). Samples were scanned  
127 at a scanning rate of 4°/min.

## 128 **2.6. Assessment of antimicrobial assay**

### 129 **2.6.1. Antibacterial activity of nanoparticles formulations**

130 The antibacterial activity of the nanoparticles was evaluated against *P. carotovra* and *R.*  
131 *solaniserum* by the agar diffusion method with LB agar media. A 20 mL of LB agar media was  
132 poured into sterilized petri dishes and the plates were leaved for solidification then bacterial  
133 suspension of the two tested bacteria was streaked. The paper discs of 6 mm size were saturated  
134 with 20  $\mu\text{L}$  of silver nanoparticles solutions (100, 200, 400 and 600 mg/L) or Doxycycline (30  
135  $\mu\text{g}$ ) as standard antibacterial agent and plated on the surface of each plates at equivalent distance  
136 with control. Bacteria was stand by 30 min, then incubated at 30° C for 24 h and the formed  
137 inhibition zone was measured and three replicates were used (**Abbassy et al., 2016**).

### 138 **2.6.2. Antifungal activity of nanoparticles formulations**

139 The antifungal activity was tested using mycelia radial growth technique (**Badawy et al.,**  
140 **2014**). The compounds were dissolved and serial concentrations ranged from 1000 to 3000 mg/L  
141 were tested. **Standard fungicide, gold plus** was used at 0.25, 0.5 and 1.0 fold of field application  
142 (200 g/100 L). The aliquots of the stock solutions were added to the PDA medium, and then  
143 transferred to Petri dishes. After solidification, the mixtures were inoculated with a 5 mm in

144 diameter mycelium fungi at the center of Petri dishes and these were incubated in the dark at 27  
145  $\pm$  2°C. Fungal growth was measured when the control had grown to the edge of the plate. The  
146 inhibition of fungal growth was calculated as the percentage of inhibition of radial growth  
147 compared to the control. The effective concentration that inhibits 50% of mycelial growth (EC<sub>50</sub>)  
148 for each compound was estimated by probit analysis (**Finney 1971**) using SPSS 21.0 software.

## 149 **2.7. Molecular identification of obtained isolates using specific PCR, sequencing and** 150 **phylogenetic analysis**

151 DNA was isolated from the two bacterial isolates and the fungus isolate using QIAgene  
152 DNA extraction kit according to the manufacture procedures (QIAgene, Germany). PCR  
153 amplification for the bacteria was performed using the 16S rRNA primers (forward;  
154 AGAGTTTGATCCTGGCTCAG and reverse; AAGGAGGTGATGCAGCC) according to  
155 (**weisburg et al., 1991**). On the other hand, the fungus DNA was subjected to PCR amplification  
156 using ITS specific primers (ITS1; TCCGTAGGTGAACCTGCGG and ITS4;  
157 TCCTCCGCTTATTGATATG) according to (**White et al., 1990**). The 25  $\mu$ L PCR reaction  
158 components were; 12.5  $\mu$ L master mix (Applied Biotechnology, Egypt), 1  $\mu$ L DNA (30 ng),  
159 1  $\mu$ L for each primer (10 p mol/ $\mu$ L) and the volume completed up to 25  $\mu$ L with sterile H<sub>2</sub>O.  
160 The PCR program was applied as follow; initial denaturation at 95°C for 2 min; 34 cycles of  
161 94°C for 1 min; annealing at 55°C for 1 min; extension at 72°C for 1 min and a final extension  
162 step at 72°C for 5 min; A 5  $\mu$ L of PCR products were separated on 2% (w/v) agarose gel  
163 electrophoresis in 0.5x TBE buffer. The molecular weight of band was estimated using DNA  
164 marker. Finally, the gel was photographed using gel documentation system. PCR products were  
165 purified using PCR clean up column kit (Maxim biotech INC, USA). The purified PCR products  
166 were subjected to DNA sequencing using the forward primer of 16S rRNA and ITS (Sigma  
167 company, Korea). The DNA nucleotide sequences were alignment using BLASTn  
168 (<http://www.ncbi.nlm.gov/BLAST>) and then the clean sequences was submitted to Gene Bank.  
169 Phylogenetic tree was constructed using Mega 4 program, to examine the origin of the obtained  
170 microbial strains (**Tamura et al., 2007**).

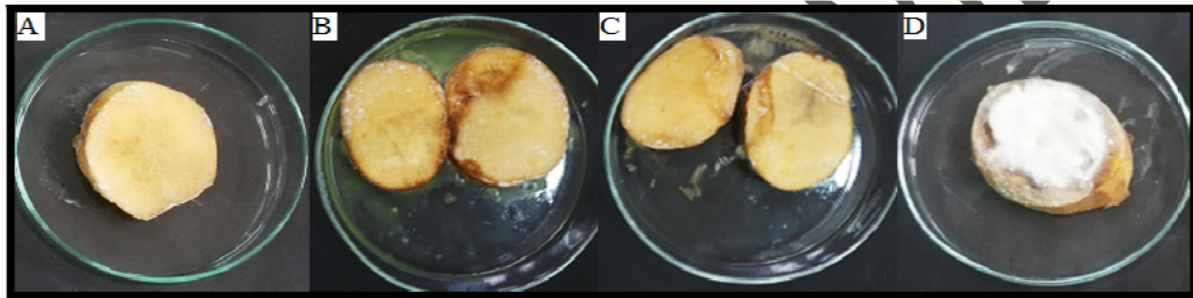
## 171 **2.8. Statistical analysis**

172 Statistical analysis was performed using SPSS 21.0 software (Statistical Package for Social  
173 Sciences, USA). All experiments were repeated at least 3 times. The data were expressed as the  
174 mean  $\pm$  standard error (SE). The log dose-response curves allowed determination of the EC<sub>50</sub>  
175 values for the fungal bioassay according to the probit analysis (**Finney 1971**). The 95%  
176 confidence limits for the range of EC<sub>50</sub> values were determined by the least-square regression  
177 analysis of the relative growth rate (% control) against the logarithm of the compound  
178 concentration.

## 179 **3. Results and Discussion**

### 180 **3.1. Pathogenicity test**

181 Many different bacteria and fungi were successfully isolated from collected potato tuber,  
182 they include; *P. carotovra*, *R. solaniserum* and *F. oxysporum*, all of which were implicated as  
183 pathogens when tested on healthy tubers. The bacterial isolate showed high capability for  
184 infection the healthy potato tubers. *P. carotovra* causes soft rot disease symptoms in the  
185 inoculated healthy potato tubers after 4-5 days post inoculation. The appeared symptoms were;  
186 chlorosis, wilting, tuber rot, blackleg and haulm desiccation. These results are in agreement with  
187 those obtained by **Motyka et al., (2017) and Onkendi and Moleleki, (2014)**. While, healthy  
188 potato tuber inoculated with *R. solanacearum* was showed the wilt disease symptoms; vascular  
189 browning, dark brown streaks and grey-white bacterial ooze was observed on tuber surfaces.  
190 Moreover, the *F. oxysporium* was isolated and used in inoculation of the healthy tubers and it  
191 was observed that the isolate succeeded to cause dry rot disease for the tubers after 7 days. The  
192 observed symptoms were; dry rot, sunken, wrinkled and a white mold was visible on tuber  
193 surfaces (**Fig. 1**).

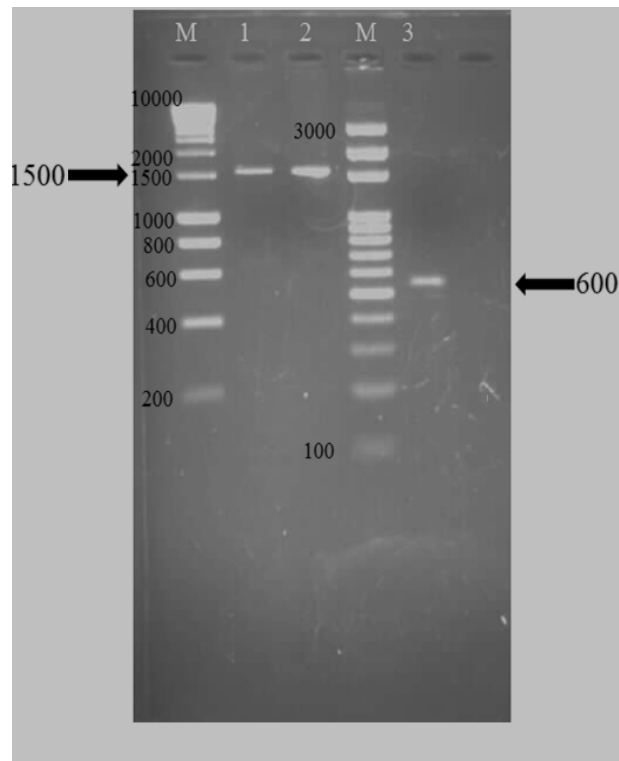


194  
195 **Fig. 1:** Pathogenicity test of the potato tubers. Tuber control (A); tuber infected with *P. carotovra*  
196 (B); tuber infected with *R. solanacearum* (C) and tuber infected with *F. oxysporium* (D).

### 197 3.2. Molecular identification of the obtained isolates

198 Approximately 1500 bp region of the 16SrRNA gene was amplified for *P. carotovra* and *R.*  
199 *solanacearum*, while, PCR product of ITS gene amplified 550 bp for *F. oxysporium* (**Fig. 2**)  
200 using universal primers. The DNA sequence results revealed that the examined two bacteria and  
201 one isolate of fungi. The phylogentic tree constructed based on the obtained DNA sequence  
202 revealed that *P. carotovra* contained of two cluster; cluster one was divided into two sub cluster,  
203 sub cluster one was divided into two group, group one divided to two sub group which contain *P.*  
204 *carotovra* that similar with investigated isolate with different percentage. *R. solanacearum* had  
205 phylogenetic tree contained two cluster; cluster one contain *R. solanacearum* isolate whereas  
206 cluster two consist two sub cluster that divided into two group which divided into two sub group  
207 that contain different strains of *R. solanacearum*. The phylogenetic tree of *F. oxysporium*  
208 contains two cluster; cluster one divided to two sub cluster, sub cluster one contain to two group  
209 that divided into two sub group which contain strains of *F. oxysporium*. While cluster two  
210 contain two sub cluster, cluster two divided into two group, group two contain two sub group  
211 while sub group two contain detected isolate of Fusarium as shown in **Fig. (3)**.

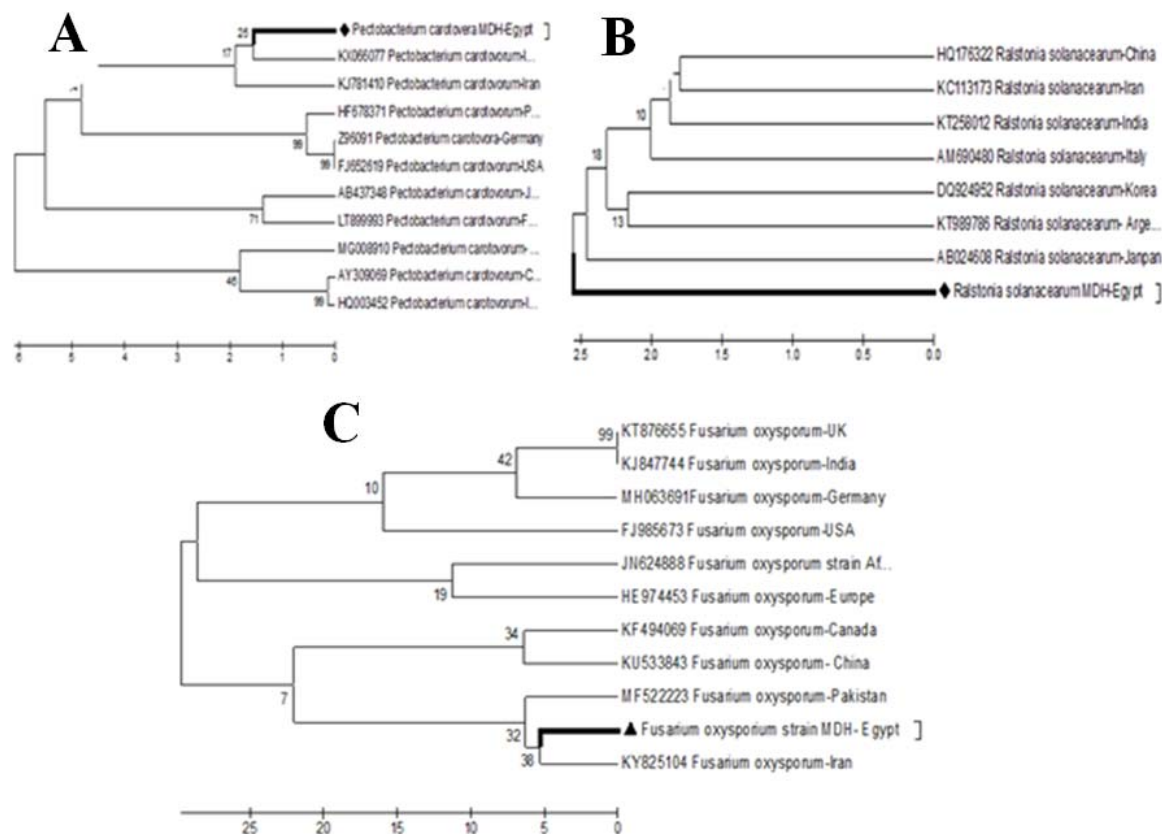
212



213

214 **Fig. 2:** PCR products of 16s RNA gene for both two bacterial isolates and iTs gene of fungi,  
 215 respectively. M, 10000 Kbp DNA marker; Lane 1, *P. carotovra*; Lane 2, *R. solanacearum*; M,  
 216 3000 Kbp DNA marker; *F. oxysporium*

217



218  
 219 **Fig. 3:** Phylogenetic tree of 16s RNA and ITS genes: *P. carotovora* (A); *R. solanacearum* (B) and  
 220 *F. oxysporium* (C). Based on the DNA nucleotide sequencing and comparing with the other  
 221 species listed in the Gene Bank.

### 222 3.3. Green synthesis of silver nanoparticles using plant extracts

223 The synthesized nanoparticles using the five different aqueous plant extracts; *M. oleifera*  
 224 (leaves) *S. nigrum* (fruits) and *P. peruviana* (leaves, red and green fruits) were obtained after  
 225 incubation period lasts for 24h. It was observed that the solution color changed from yellow to  
 226 dark brown within the first 10 hrs. Silver nanoparticles exhibit yellowish brown color in aqueous  
 227 solution due to excitation of surface plasmon vibrations in silver nanoparticles. Thus, plant  
 228 extracts act as reducing agents as well as capping agents.

229 The papaya fruit extract was mixed in the aqueous solution of the silver ion complex; it  
 230 started to change the color from watery to yellowish brown due to reduction of silver ion, which  
 231 indicated formation of silver nanoparticles (Jain et al., 2009). UV-Vis spectroscopy could be  
 232 used to examine size- and shape-controlled nanoparticles in aqueous suspensions. Five plant leaf  
 233 extracts (Pine, Persimmon, Ginkgo, Magnolia and Platanus) were used and compared for their  
 234 extracellular synthesis of silver nanoparticles (Song and Kim, 2009). Stable silver nanoparticles  
 235 were formed by treating aqueous solution of  $\text{AgNO}_3$  with the plant leaf extracts as reducing  
 236 agent of  $\text{Ag}^+$  to  $\text{Ag}^0$ . Magnolia leaf broth was the best reducing agent in terms of synthesis rate



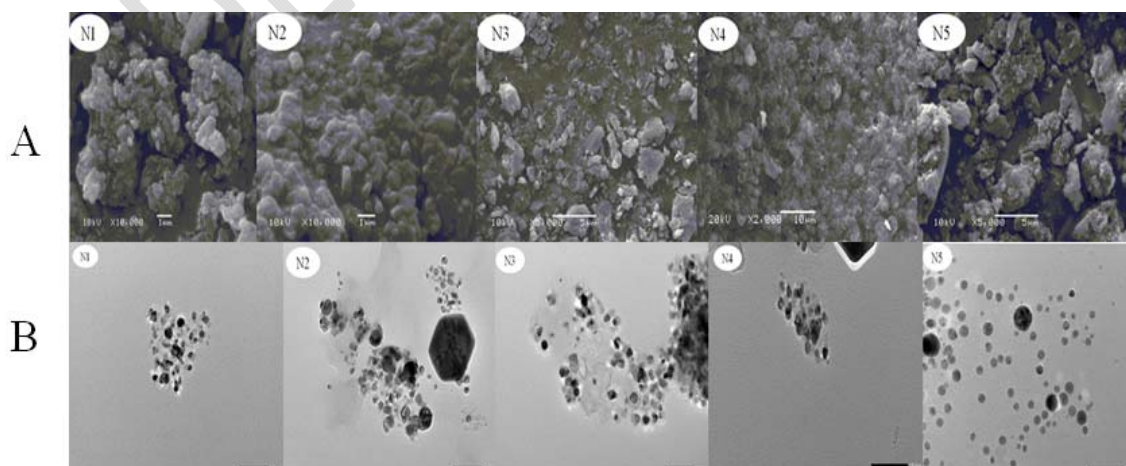
237 and conversion to silver nanoparticles. The average particle size ranged from 15 to 500 nm.  
238 Silver nanoparticles were rapidly synthesized using leaf extract of *Acalypha indica* and the  
239 formation of nanoparticles was observed within 30 min with the size of 20–30 nm (**Krishnaraj**  
240 **et al., 2010**). **Ali et al., (2011)** showed that the leaf extract of menthol is very good bioreductant  
241 for the synthesis of silver nanoparticles and synthesized nanoparticles were found to be spherical  
242 in shape with 90 nm.

### 243 3.4. Characterization of silver nanoparticles formulations

244 The obtained silver nanoparticles was subjected to different characterization methods; SEM,  
245 TEM, XRD and FT-IR. From the SEM and TEM micrograph of AgNPs, different extracts  
246 produce different size and different crystals, which occurs different effective of the activity of  
247 nanoparticles on organisms (**Figs. 4A and 4B**). FT-IR results revealed that the obtained particles  
248 are silver nanoparticles when compared with the standard nanosilver profile (**Fig. 5A**). It was  
249 noticed that extract which produced silver nanoparticles in the rage of 12-33 nm, and detected  
250 the function group which coated on the surface of particles by X-RD and FT-IR.

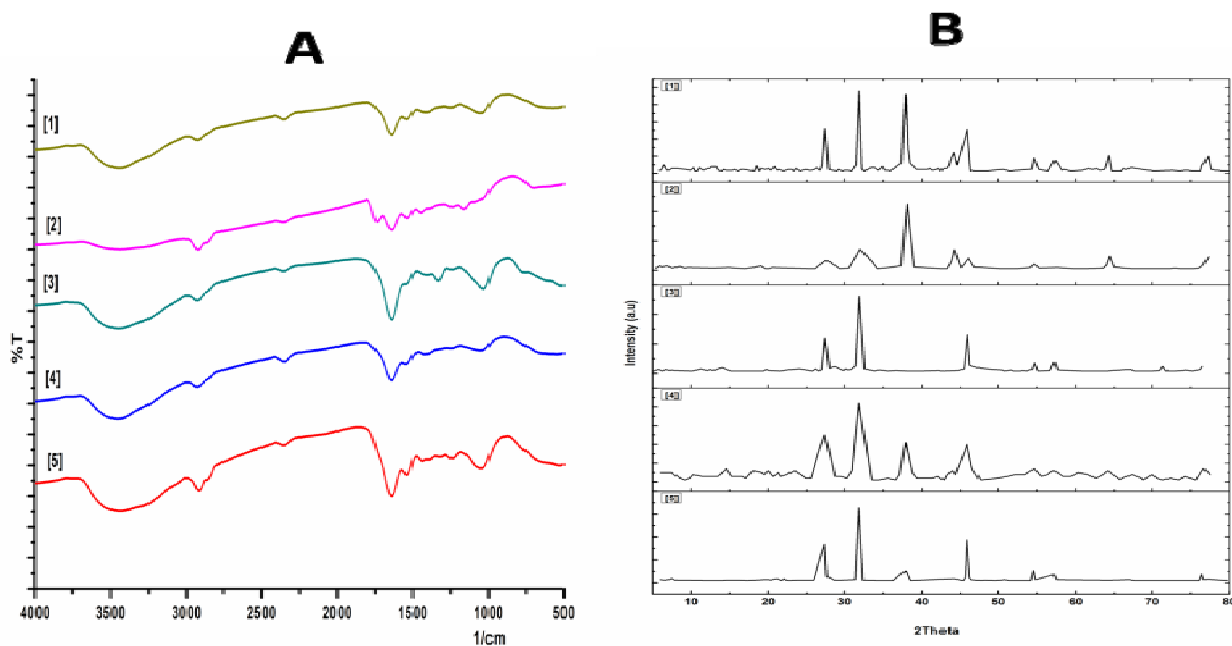
251 The biosynthesised silver nanoparticles by using papaya fruit extract was confirmed by XRD  
252 and SEM (**Jain et al., 2009**). The characteristic peaks observed in the XRD image showed in  
253 (**Fig. 5B**) three intense peaks in the whole spectrum of  $2\theta$  value ranging from 10 to 80. The XRD  
254 pattern average size of the particles synthesized was 15 nm with size range 10 to 50 nm with  
255 cubic and hexagonal shape. The SEM image showing the high-density silver nanoparticles  
256 synthesized by the papaya extract further confirmed the development of silver nanostructures.

257 FT-IR analysis was used for the characterization of the extract and the resulting  
258 nanoparticles (**Bar et al., 2009**). The  $1226\text{ cm}^{-1}$  band arises most probably from the C–O group  
259 of polyols such as hydroxyflavones and catechins. The total disappearance of this band after the  
260 bioreduction may be due to the fact that the polyols are mainly responsible for the reduction of  
261 Ag ions, whereby they themselves get oxidized to unsaturated carbonyl groups leading to a broad  
262 peak at  $1650\text{ cm}^{-1}$  (for reduction of Ag) (**Jain et al., 2009**).



263

264 **Fig. 4:** SEM (A) and TEM (B) of silver nanoparticles formulations, N1 to N5. The SEM was  
265 performed on a JEOL JSM-1200EX II scanning electron microscope operating at an acceleration  
266 voltage of 80.0 kV with 20  $\mu\text{m}$  aperture.  
267



268  
269 **Fig. 5 :** The FT-IR spectra (A) of the five biosynthesized silver nanoparticles and the XRD (B)  
270 analysis of the five biosynthesized silver nanoparticles: *S. nigrum* (1); *P. peruviana* Red (2);  
271 Leave *P. peruviana* (3); Green *P. peruviana* (4); *M. oliefera* (5).

### 272 3.5. Antibacterial activity of silver nanoparticles formulations

273 The *in vitro* antibacterial activity of silver nanoparticles formulations against *R.*  
274 *solanacearum* and *P. carotovra* is presented in Table 1 using the agar diffusion method. The  
275 measured zone of inhibition of the silver nanoparticles formulations showed significantly  
276 different inhibitory effects. The results demonstrated that all formulations showed good  
277 inhibition (Inhibition (%)) ranged from 20.56 to 29.26 %) against the tested bacteria and the  
278 inhibitory effects were concentrations dependent. For the five silver nanoparticles formulations,  
279 N5 formulation exerted significantly potent antibacterial activity against *R. solanacearum*.  
280 Followed by N4 in the descending order. However, N1 formulation was the lowest active as  
281 showed in Fig. 6. Against *P. carotovra*, N1 formulation exerted significantly potent antibacterial  
282 activity. Followed by N5 in the descending order. However, N4 formulation was the lowest  
283 active as showed in Fig. 6. When we consider the susceptibility of the microorganisms, another  
284 point deserves attention; it can be noticed that bacterium of *P. carotovra* was more susceptible  
285 than *R. solanacearum* to all formulations (Table 1 and Fig. 6). It appears that the antibacterial

286 activity of the silver nanoparticles formulations increased with increase in surface-to-volume  
 287 ratio, due to the decrease in size of nanoparticles.

288 Antibacterial effects of Ag nanoparticles obeyed a dual action mechanism of antibacterial  
 289 activity, i.e., the bactericidal effect of Ag<sup>+</sup> and membrane-disrupting effect of the polymer  
 290 subunits. The antibacterial activities of Ag nanoparticles, Ag<sup>+</sup> ions were blocked by  
 291 thiolcontaining agents. Silver was also known to cause pits in bacterial cell walls, leading to an  
 292 increased cell-membrane permeability and cell death (Sambhy et al., 2006). The antibacterial  
 293 activity of synthesized silver nanoparticles using leaf extract of *Acalypha indica* showed  
 294 effective inhibitory activity against water borne pathogens, *Escherichia coli* and *Vibrio cholera*  
 295 (Krishnaraj et al., 2010). Silver nanoparticles 10 g/ml were recorded as the minimal inhibitory  
 296 concentration (MIC) against *E. coli* and *V. cholerae*. Alteration in membrane permeability and  
 297 respiration of the silver nanoparticle treated bacterial cells were evident from the activity of  
 298 silver nanoparticles.

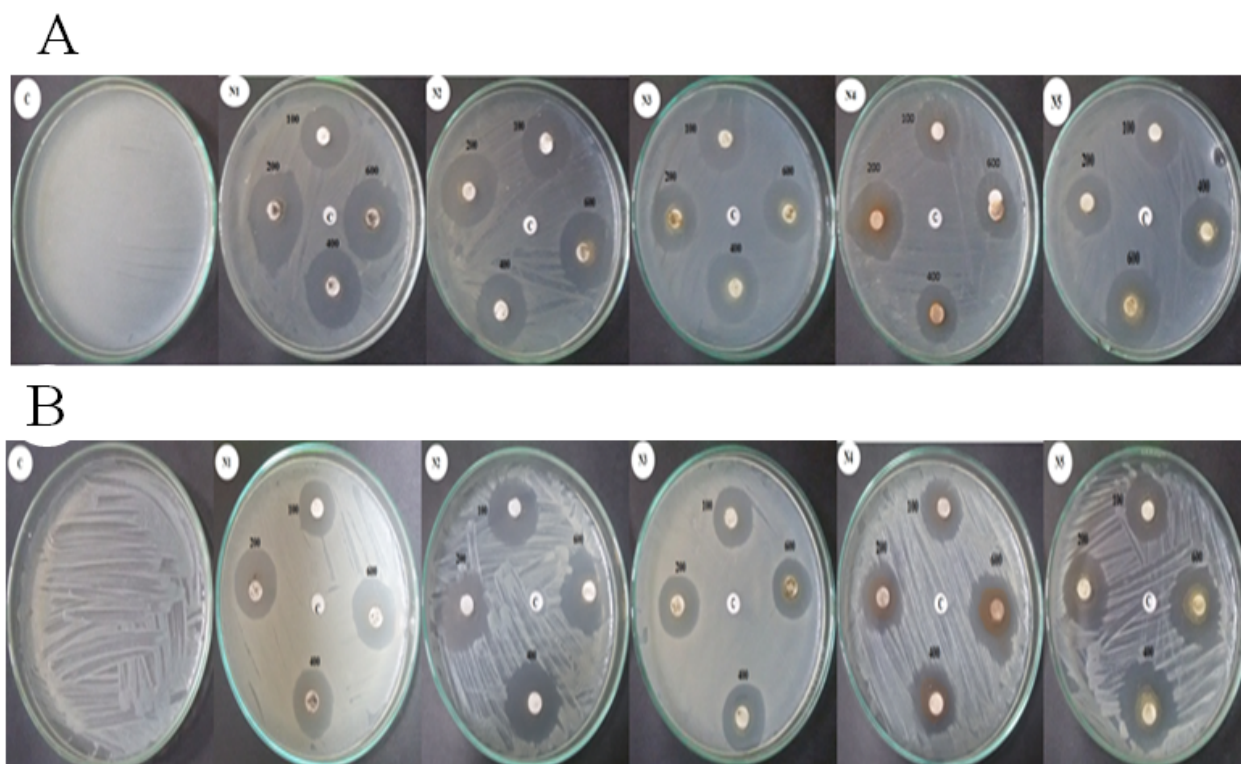
299 **Table 1:** The *in vitro* antibacterial activity of biosynthesized silver nanoparticles against *R.*  
 300 *solanacearum* and *P. carotovra* by the agar diffusion method

Formulations	Conc. (mg/L)	Inhibition (%)	
		<i>R. solanacearum</i>	<i>P. carotovra</i>
N1	100	20.95 ± 1.39	23.70 ± 0.64
	200	21.48 ± 0.64	24.81 ± 1.70
	400	21.48 ± 2.24	27.04 ± 1.70
	600	22.22 ± 1.46	29.26 ± 0.64
N2	100	20.56 ± 1.11	21.07 ± 1.11
	200	23.04 ± 1.79	23.37 ± 1.89
	400	23.14 ± 2.62	25.9 ± 2.79
	600	24.63 ± 2.50	26.26 ± 1.45
N3	100	22.04 ± 0.32	23.70 ± 1.69
	200	22.96 ± 1.69	24.07 ± 1.89
	400	23.15 ± 1.15	25.00 ± 0.56
	600	23.26 ± 1.67	25.22 ± 0.91
N4	100	20.74 ± 2.56	16.85 ± 6.62
	200	21.85 ± 2.56	22.22 ± 3.33
	400	22.04 ± 4.01	22.59 ± 0.64
	600	25.00 ± 1.11	23.89 ± 2.00
N5	100	22.41 ± 0.32	21.85 ± 0.84
	200	26.30 ± 2.74	23.15 ± 1.60
	400	26.67 ± 1.11	26.67 ± 1.11
	600	27.04 ± 0.64	28.52 ± 2.31
Doxycycline	30	12.77 ± 0.40	22.89 ± 0.99

301

302 Green *P. peruviana* (N1); Red *P. peruviana* (N2); leaves of *P. peruviana* (N3); *S. nigrum* (N4)  
303 and *M. oliefera* (N5).

304



305

306 **Fig. 6:** The *in vitro* antibacterial activity of silver nanoparticles formulations against *P.*  
307 *carotovra* (A) and *R. solanacearum* (B) by the agar diffusion method with different  
308 concentrations (0, 100, 200, 400 and 600 mg/L, respectively). Green *P. peruviana* (N1); Red  
309 *P. peruviana* (N2); leaves of *P. peruviana* (N3); *S. nigrum* (N4) and *M. oliefera* (N5).

### 310 3.6. Antifungal activity of silver nanoparticles synthesized with plant extracts

311 The *in vitro* antifungal activity of silver nanoparticles formulations against the plant  
312 pathogenic fungus *F. oxysporum* is presented in Table 2 and the results are expressed as EC<sub>50</sub>.  
313 Most of the tested compounds showed inhibitory effect against tested fungus. For the five silver  
314 nanoparticles formulations, N1 formulation exerted significantly potent antifungal activity with  
315 EC<sub>50</sub> of 687.03 mg/L against *F. oxysporum*. Followed by N3 in the descending order with EC<sub>50</sub>  
316 of 981.61 mg/L. However, N2 formulation was the lowest active (EC<sub>50</sub> = 1474.86 mg/L against  
317 tested fungus as showed in Fig. 7. Standard fungicide, Ridomil gold showed the highest  
318 fungicidal activity (EC<sub>50</sub> = 204.02 mg/L). From statistical analysis, there is no significant  
319 difference between standard fungicide and N1 formulation (see Table 2).

320 Different concentrations of biosynthesized silver nanoparticles were tested to know the  
321 inhibitory effect of fungal plant pathogens namely *Alternaria alternata*, *Sclerotinia sclerotiorum*,

322 *Macrophomina phaseolina*, *Rhizoctonia solani*, *Botrytis cinerea* and *Curvularia lunata*.  
 323 Remarkably, 15 mg concentration of silver nanoparticles showed excellent inhibitory activity  
 324 against all the tested pathogens (Krishnaraj et al., 2012). Rajiv et al., (2013) synthesized  
 325 different sized zinc oxide nanoparticles and explored the size-dependent antifungal activity  
 326 against plant fungal pathogens. Highest zone of inhibition was observed in 25 µg/ml of  
 327 27 ± 5 nm size zinc oxide nanoparticles against *Aspergillus flavus* and *Aspergillus niger*.  
 328 Narayanan and Park, (2014) demonstrated the synthesis of silver nanoparticles using turnip  
 329 leaf extract and its interaction with wood-degrading fungal pathogens, *Gloeophyllum abietinum*,  
 330 *G. trabeum*, *Chaetomium globosum*, and *Phanerochaete sordida*. The synthesized silver  
 331 nanoparticles showed broad-spectrum antifungal activity against wood-degrading fungi by  
 332 inhibiting growth.

333 Reports on the mechanism of inhibitory action of silver ions on microorganisms have shown  
 334 that upon treatment with Ag<sup>+</sup>, DNA loses its ability to replicate resulting in inactivated  
 335 expression of ribosomal subunit proteins, as well as certain other cellular proteins and enzymes  
 336 essential to ATP production (Feng et al., 2000; Yamanaka et al., 2005). It has also been  
 337 hypothesized that Ag<sup>+</sup> primarily affects the function of membrane-bound enzymes, such as those  
 338 in the respiratory chain (McDonnell and Russell, 1999).

339  
 340 **Table 2.** The *in vitro* antifungal activity of biosynthesized silver nanoparticles against *F.*  
 341 *oxysporium* by mycelia radial growth technique.

Formulations	EC <sub>50</sub> <sup>a</sup> (mg/L)	95% confidence limits		Slope <sup>b</sup> ± SE	Intercept <sup>c</sup> ± SE	(χ <sup>2</sup> ) <sup>d</sup>
		Lower	Upper			
N1	687.03	39.36	687.03	1.588±0.602	-4.419±1.945	0.412
N2	1474.86	1087.44	1709.49	1.942±0.567	-6.153±1.838	1.829
N3	981.61	99.52	1321.13	1.404±0.572	-4.200±1.853	0.269
N4	1319.49	685.56	1588.39	1.629±0.566	-5.08±1.833	0.030
N5	999.61	257.19	1306.04	1.596±0.576	-4.788±1.866	0.780
<b>Ridomil gold</b>	204.02	138.44	680.25	0.976±0.305	-2.255±0.618	0.575

343 <sup>a</sup>The concentration causing 50% mycelial growth inhibition.

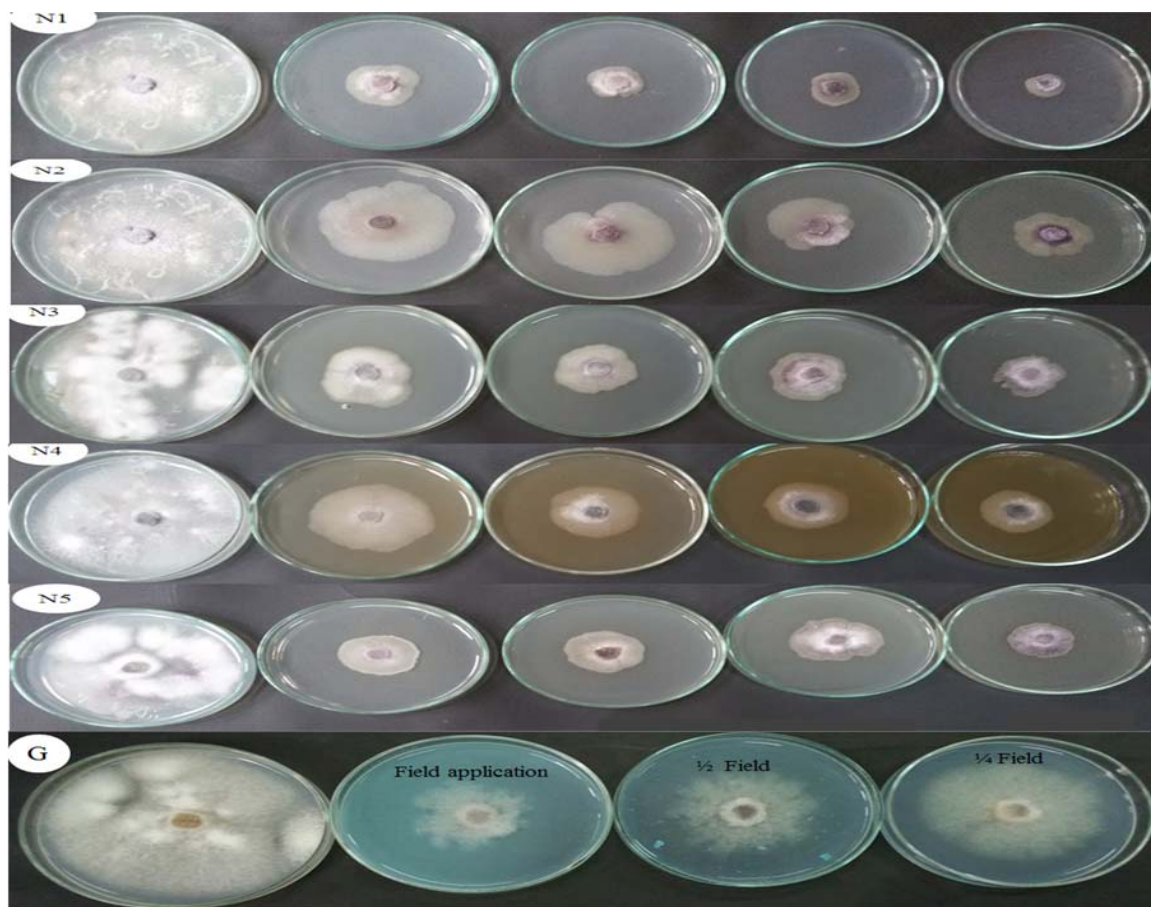
344 <sup>b</sup>Slope of the concentration-inhibition regression line ± standard error.

345 <sup>c</sup>Intercept of the regression line ± standard error.

346 <sup>d</sup>Chi square value.

347 Green *P. peruviana* (N1); Red *P. peruviana* (N2); leaves of *P. peruviana* (N3); *S. nigrum* (N4)  
 348 and *M. oliefera* (N5).

349



350  
351

352 **Fig. 7:** The antifungal activity of the silver nanoparticles formulations (from left to right, 0,  
353 1200, 1600, 2000 and 2400 mg/L, respectively) against *F. oxysporium*. Green *P. peruviana* (N1);  
354 Red *P. peruviana* (N2); leaves of *P. peruviana* (N3); *S. nigrum* (N4) and *M. oliefera* (N5);  
355 Ridomil gold (G)

356

### 357 References

358 **Abbassy, M.A., Masoud, S.A., and Nassar, A.M.K.** (2016). In vitro antibacterial activity and  
359 phytochemical analysis of *abrus precatorius* linn. *Egy. J. Plant Pro. Res*, 4 (2), 1-14.

360 **Ali, D.M., Thajuddin, N., and Jeganathan, K.** (2011). Plant extract mediated synthesis of  
361 silver and gold nanoparticles and its antibacterial activity against clinically isolated  
362 pathogens. *Colloids and Surfaces B: Biointerfaces*, (85), 360-365.

363 **Aliye, N., Fininsa, C., and Hiskias, Y.** (2008). Evaluation of rhizosphere bacterial antagonists  
364 for their potential to bioprotect potato (*Solanum tuberosum*) against bacterial wilt  
365 (*Ralstonia solanacearum*). *Biological Control*, 47, 282-288.

- 366 **Badawy, M.E.I., Rabea, E.I., and Taktak, N.E.M.** (2014). Antimicrobial and inhibitory  
367 enzyme activity of N-(benzyl) and quaternary N-(benzyl) chitosan derivatives on plant  
368 pathogens. *Carbohydrate polymers*, 111, 670-682.
- 369 **Banerjee, P., Satapathy, M., Mukhopahayay, A., and Das, P.** (2014). Leaf extract mediated  
370 green synthesis of silver nanoparticles from widely available Indian plants: synthesis,  
371 characterization, antimicrobial property and toxicity analysis: *Bioresources and*  
372 *Bioprocessing*. 1:3.
- 373 **Bar, H., Bhui, D.K., Sahoo, G. P., Sarkar, P., De, S.P., and Misra, A.** (2009). Green synthesis  
374 of silver nanoparticles using latex of *Jatropha curcas*. *Colloids and Surfaces A.*  
375 *Physicochemical and Engineering Aspects*, (339), 134-139.
- 376 **Belosokhov, A. F., Belov, G. L., Chudinova, E. M., L.YU. Kokaeva, L. Y., and ELansky, S.**  
377 **N.** (2017) *Alternaria spp.* and *Colletotrichum coccodes* in potato leaves with early  
378 blight symptoms. *PAGV – SPECIAL REPORT*, 18, 181-190.
- 379 **Dees, M.W., Lebecka, R., Perminow, J.I.S., Czajkowski, R., Grupa, A., Motyka, A.,**  
380 **Zoledowska, S., Śliwka, J., Lojkowska, E., and Brurberg, M. B.** (2017).  
381 Characterization of *Dickeya* and *Pectobacterium* strains obtained from diseased potato  
382 plants in different climatic conditions of Norway and Poland. *Eur J Plant Pathol*  
383 ,(148),839–851.
- 384 **Douches, D.S., Jastrzebski, K., Maas, D., and Chase, R.W.** (1996). Assessment of potato  
385 breeding over the past century. *Crop Science*, 36, 1544-1552.
- 386 **Feng, Q.L., Wu, J., Chen, G. Q., Cui, F.Z., Kim, T.N., and Kim, J.O.** (2000). A mechanistic  
387 study of the antibacterial effect of silver ions on *Escherichia coli* and *Staphylococcus*  
388 *aureus*. *National Natural Science Foundation of China*,(52), 662-668.
- 389 **Finney, D. J.** (1971). Statistical Logic in the Monitoring of Reactions to Therapeutic Drugs.  
390 *Methods Inf Med*, 10(04), 237-245.
- 391 **Haverkort, A.J.** (1990). Ecology of potato cropping system in relation to latitude and altitude.  
392 *Agricultural Systems*, 32 (3), 251-272.
- 393 **Jain, J., Arora, S., Rajwade, J. M., Omray, P., Khandelwal, S., and Paknikar, K.M.** (2009).  
394 Silver Nanoparticles in Therapeutics: Development of an Antimicrobial Gel  
395 Formulation for Topical Use. *Molecular Pharmaceutics*, 6 (5), 1388–1401.
- 396 **Kelman, A.** (1954) The Relationship of the Pathogenicity of *Pseudomonas solanacearum* to  
397 Colony Appearance on a Tetrazolium Medium. *Phytopathology*, 44, 693-695.
- 398 **Krishnaraj, C., Jagan, E. G., Rajasekar, S., Selvankumar, P., Kalaichelvan, P.T., and**  
399 **Mohan, N.** (2010). Synthesis of silver nanoparticles using *Acalypha indica* leaf extracts  
400 and its antibacterial activity against water borne pathogens. *Colloids and Surfaces B:*  
401 *Biointerfaces*, (76), 50-56.

- 402 **Krishnaraj, C., JaganS, E. G., Selvakumar, R.P., Kalaichelvan, P.T., and Mohan,N.** (2010).  
403 Synthesis of silver nanoparticles using *Acalypha indica* leaf extracts and its antibacterial  
404 activity against water borne pathogens. *Colloids and Surfaces B: Biointerfaces*, (76), 50-  
405 56.
- 406 **Krishnaraj, C., Ramachandran, R., Mohan, K., and Kalaichelvan, P.T.** (2012). Optimization  
407 for rapid synthesis of silver nanoparticles and its effect on phytopathogenic fungi.  
408 *Spectrochimica Acta Part A. Molecular and Biomolecular Spectroscopy*, (93), 95-99.
- 409 **Leite, L.N., de Haan, E.G., Krijger, M., Kastelein, P., der Zouwen, P. S. V., den**  
410 **Bovenkamp, G. W. V., Tebaldi, N. D., and der Wolf, J. M. V.** (2014). First report of  
411 potato blackleg caused by *Pectobacterium carotovorum* subsp. *brasiliensis* in the  
412 Netherlands. *New Disease Reports*, 29,24.
- 413 **Lo'pez, M. M., and Biosca, E. G.** (2004) Potato bacterial wilt management: new prospects for  
414 an old problem. In Allen, C., Prior, P., and Hayward C. *Bacterial wilt disease and the*  
415 *Ralstonia solanacearum* species complex. APS Press, St. Paul, Minnesota, USA, 205-  
416 224.
- 417 **Maniatis, T., Fritsh, E.F., and Sambrook, J.** (1982) *Molecular cloning: a laboratory manual.*  
418 Cold Spring Harbor Laboratory, Cold Spring Harbor, NY
- 419 **McDonnell, G., and Russell, A.D.** (1999). Antiseptics and Disinfectants: Activity, Action, and  
420 Resistance. *American Society for Microbiology*, (12), 147–179.
- 421 **Motyka, A., Zoledowska, S., Sledz, W., and Lojkowska, E.** (2017). Molecular methods as  
422 tools to control plant diseases caused by *Dickeya* and *Pectobacterium* spp. *New*  
423 *BIOTECHNOLOGY*, 39, 181- 189.
- 424 **Narayanan, K.B., and Park, H.H.** (2014). Antifungal activity of silver nanoparticles  
425 synthesized using turnip leaf extract (*Brassica rapa L.*) against wood rotting pathogens.  
426 *Eur J Plant Pathol*, (140), 185-192.
- 427 **Okigbo, R.N., and Ogbonnaya, U.O.** (2006). Antifungal effects of two tropical plant leaf  
428 extract (*Ocimum gratissimum* and *Aframomum melegueta*) on postharvest yam  
429 (*Dioscorea spp.*) rot. *African Journal of Biotechnology*, 5(9), 727- 731.
- 430 **Onkendi, E.M., and Moleleki, L.N.** (2014). Characterization of *Pectobacterium carotovorum*  
431 subsp. *carotovorum* and *brasiliense* from diseased potatoes in Kenya. *Eur J Plant*  
432 *Pathol*, (139), 557–566.
- 433 **P. Rajiv, P., Rajeshwari, S., and Venckatesh, R.** (2013). Bio-Fabrication of zinc oxide  
434 nanoparticles using leaf extract of *Partheniumhy sterophorus L.* and its size-dependent  
435 antifungal activity against plant fungal pathogens. *Spectrochimica Acta Part A:*  
436 *Molecular andBiomolecular Spectroscopy*, 112, 384-387.
- 437 **Patil, B.M., and Hooli, A.A.** (2013). Evaluation of antibacterial activities of environmental  
438 benign synthesis of silver nanoparticles using the flower extracts of *plumeria albalinn.*



- 439 JOURNAL OF NANOSCIENCE, NANOENGINEERING & APPLICATIONS, 3, 19-  
440 33.
- 441 **Rashid, A., Fahad, M. A. B., Khan, M. A. , Mateen, A., Farooq, M., Ashraf, M.,**  
442 **Ahmad, F., and Ahmad, M.** (2012). Incidence of potato blackleg caused by  
443 *Pectobacterium atrosepticum* in district Chiniot and its management through bio-  
444 products. African Journal of Agricultural Research, 7, 6035-6048.
- 445 **Sambhy, V., MacBride, M. M., Peterson, B. R., and Sen, A.** (2006). Silver Bromide  
446 Nanoparticle/Polymer Composites: Dual Action Tunable Antimicrobial Materials. J.  
447 Am. Chem. Soc., 128 (30), 9798- 9808.
- 448 **Sambhy, V., MacBride, M.M., Peterson, B. R., and Sen, A.** (2006). Silver Bromide  
449 Nanoparticle/Polymer Composites: Dual Action Tunable Antimicrobial Materials.  
450 American Chemical Society, 128.30, 9798-9808.
- 451 **Sastry, R.K., Rashmi, H.B., and Rao, N.H.** (2010). Nanotechnology for enhancing food  
452 security in India. Food Policy, 36, 391- 400.
- 453 **Shabana, Y. M., Abdel-Fattah, G. M., Ismail, A. E., and Rashad, Y. M.** (2008). Control of  
454 brown spot pathogen of rice (*Bipolaris oryzae*) using some phenolic antioxidants.  
455 Brazilian Journal of Microbiology, 39, 438- 444.
- 456 **Shariff , N., Sudarshana, M.S., Umesha ,S., and Hariprasad, P.** (2006). Antimicrobial  
457 activity of Rauvolfia tetraphylla and Physalis minima leaf and callus extracts. Afr. J.  
458 Biotech, 5(10), 946-950.
- 459 **Song, J.Y. and Kim, S.M.** (2009). Rapid biological synthesis of silver nanoparticles using plant  
460 leaf extracts. Bioprocess Biosyst Eng, (32), 79-84.
- 461 **Tamura, K., Dudley, J., Nei, M., and Kumar, S.** (2007). MEGA4: Molecular Evolutionary  
462 Genetics Analysis (MEGA) Software Version 4.0: Molecular Biology and Evolution, (  
463 24), 1596–1599.
- 464 **Varma, J., and Dubey, N. K.** (1999). Prospective of botanical and microbial products as  
465 pesticides of Tomorrow. Current science, 76, 172-179.
- 466 **Weisbrug, W. G., Barans, S. M., Pelletier, D.A., and Lane, D. J.** (1991). 16S Ribosomal DNA  
467 amplification for phylogenetic study. Journal of Bacteriological, 173, 697-703.
- 468 **White, T.J., Bruns, T., Lee, S., and Taylor, J.W.** (1990). Amplification and direct sequencing  
469 of fungal ribosomal RNA genes for phylogenetic. In: Innis, M.A., Gelfand, D.H.,  
470 Sninsky, J.J., and White, T.J. editors. PCR protocols: a guide to methods and  
471 applications. San Diego: Academic Press, 315-22.
- 472 **Zhang, X.Y., Yu, X.X., Yu, Z., Xue, Y.F., and Qi, L.P.** (2014). A simple method based on  
473 laboratory inoculum and field inoculum for evaluating potato resistance to black scurf  
474 caused by *Rhizoctonia solan*. Breeding Science, 64, 156–163.